

Detonation propagation in the inhomogeneous mixtures with periodic reactant concentration gradient

Yuan Wang^{1,2}, Chengyang Huang¹, Haitao Chen², Zheng Chen¹

¹ SKLTCS, CAPT, BIC-ESAT, Department of Mechanics and Engineering Science, College of Engineering, Peking University, Beijing 100871, China

² Institute of Applied Physics and Computational Mathematics, Beijing 100094, China

1 Introduction

Recently, propagation of gaseous detonation in the inhomogeneous mixtures has received great attention. Such situations occur for instance in detonation engines and accidental explosions [1, 2]. In previous studies, generally, four typical distributions of inhomogeneous mixture have been considered (see Fig. 1 of [3]). Besides, detonation propagation in mixtures with randomly distributed inert regions or in a porous medium has also been investigated [4, 5]. Different from previous studies, in rotating detonation engines (RDEs), the unburned reactants are injected into the combustion chamber through injection ports and burned gas might exist at the injection-port intervals [1]. In explosion accidents, the injection of water and inert gas is used to disperse the continuous distribution of combustible gas [2]. Therefore, in both RDEs and explosion accidents, a detonation might propagate in mixtures with periodic fuel concentration gradient. However, in the literature there are only a few related studies on detonation propagation in this specific type of inhomogeneous mixture.

Thomas et al. [6] experimentally investigated detonation propagation in non-uniform mixture and found that the transmitted detonation adjusts its speed and cell size rapidly to the local gas composition. Boubal et al. [7] proposed a criterion to quantify shock-flame decoupling. Ma et al. [8] conducted one-dimensional (1D) simulations and found that a periodic gradient in reactant concentration leads to a detonation velocity deficit. Most of previous studies considered detonation propagation in mixtures with a single concentration gradient. However, detonation propagation in mixtures with periodic concentration gradient received little attention. Besides, although 1D simulation results were reported in Ma et al. [8], the evolution of cellular structure was not studied.

Based on the above considerations, here we consider detonation propagation in inhomogeneous H₂/air with periodic sinusoidal distribution of reactant concentration. 1D and two-dimensional (2D) simulations considering detailed chemistry and transport are conducted. The objective of this study is to assess the

effects of periodic distribution of reactant concentration on detonation propagation. Specifically, the detonation reinitiation, cellular structure and cell size, and detonation speed deficit have been investigated.

2 Numerical model and methods

We consider 1D and 2D detonation propagation in a stoichiometric H₂/air mixture initially at $T_0 = 300$ K and $P_0 = 1$ atm. The numerical model is sketched in Fig. 1. The ZND detonation structure was used as the initial condition. First, The detonation propagates through a static, homogeneous, stoichiometric H₂/air mixture, whose induction length is $l_i = 0.19$ mm. The length of the homogeneous mixture is about $x_0 = 315l_i$, which was chosen to ensure full development of the cellular structure for the 2D case. Then, the detonation propagates into the inhomogeneous mixture with periodic sinusoidal wave distribution of reactant concentration as shown in Fig. 1. The molar fraction of each species in inhomogeneous H₂/air mixture is:

$$\begin{aligned} x_{\text{H}_2} &= \{2 - 2 \times a \times \sin[2\pi(x - x_0) / L]\} / (2 + 1 + 3.76) \\ x_{\text{O}_2} &= \{1 - 1 \times a \times \sin[2\pi(x - x_0) / L]\} / (2 + 1 + 3.76) \\ x_{\text{N}_2} &= \{3.76 + 3 \times a \times \sin[2\pi(x - x_0) / L]\} / (2 + 1 + 3.76) \end{aligned} \quad (1)$$

where L is the wavelength and a is the amplitude of the sinusoidal distribution, as depicted in Fig. 1. Equation (1) indicates that the molar ratio between hydrogen and oxygen is 2 everywhere and that the averaged fuel concentration in the inhomogeneous mixture is the same as that in the homogeneous mixture. Different values for L in the range of 1~16 mm and for a in the range of 0~1 were considered. The homogeneous mixture is recovered for $a = 0$.

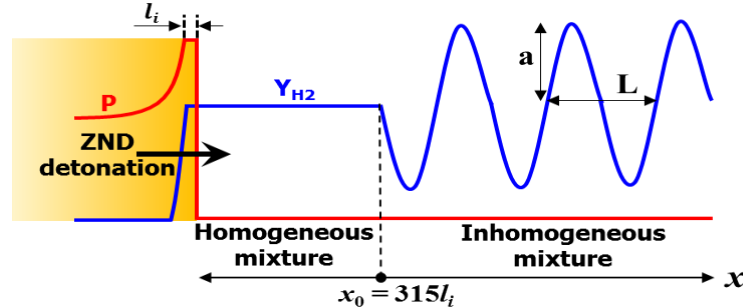


Figure 1. Schematic of the initial pressure and hydrogen mass fraction distributions

The in-house code A-SURF [9] and the parallel block-structured mesh refinement framework AMROC [10] are respectively used to simulate 1D and 2D detonation propagation in H₂/air mixture. The conservation equations for unsteady, compressible, reactive flow are solved in A-SURF and AMROC using finite volume method. Diffusion terms are kept in the conservation equations. The CHEMKIN package is used to evaluate the thermodynamic, transport properties and reaction rates. The hydrogen chemistry was used in 1D and 2D cases. In order to accurately and efficiently resolve the propagation of shock wave and detonation, dynamically adaptive mesh refinement technology is adopted in simulation. The finest mesh size is 3.9 μm and thus there is more than 40 grids within one induction length. Numerical convergence has been checked and ensured by further decreasing the time step and mesh size in simulation. Both the A-SURF and AMROC were successfully used in previous studies on detonation initiation and propagation [9, 10]. The details on governing equations and numerical schemes of A-SURF and AMROC can be found in [9, 10].

3 Results and discussion

3.1 One-dimensional detonation propagation

First we consider 1D detonation propagation in the inhomogeneous mixture. Figure 2 shows the evolution of the pressure after the leading shock. The number, n , from 1 to 7, represents the n^{th} period of sinusoidal distribution; and the minus and plus represent, respectively, lower and higher chemical reactivity than the homogeneous mixture (see Fig. 1). Fig. 2(a) shows that for a fixed wavelength $L = 16$ mm, detonation propagates with periodic fluctuations of pressure after the shock in the inhomogeneous mixture with amplitude of $a = 0.2$. For $a = 0.5$, the pressure after the shock decreases rapidly during it propagates in the region 1-. The leading shock decouples from the reaction front and thereby the detonation quenches. When the leading shock propagates into the region 1+, local autoignition occurs around $x = 9.2$ cm, where the highest concentration of H_2/O_2 appears. Then the sequential autoignition events are induced in the green zone marked in Fig. 2(a). Consequently, the reaction front accelerates and subsequently catches up and couples with the leading shock, resulting in an abrupt increase in the leading shock pressure to 70 atm. An overdriven detonation is formed and it decays to a CJ detonation at the end of region 1+. From region 2 to 7, the shock pressure is shown to change periodically with the sinusoidal distribution of reactant concentration. Moreover, after the detonation reinitiation is achieved, the variations of pressure after the shock become regular and the consecutive pressure peak is at a constant distance of $L_1 = 2L = 32$ mm. Further increase the amplitude to $a = 0.8$, leading shock pressure attenuates periodically and detonation quenches in the inhomogeneous region. Similar phenomena are observed for detonation propagating for a fixed amplitude of $a = 0.3$ but different wavelengths of $L = 2, 8$ and 16 mm. Therefore, successful detonation propagation is observed for small values of wavelength and amplitude.

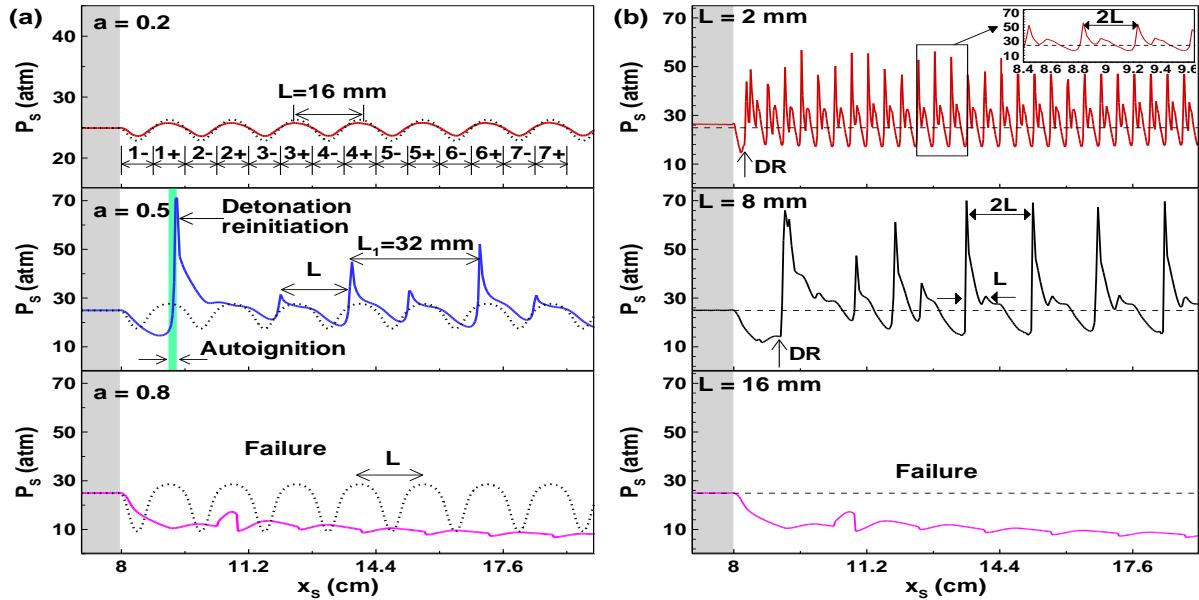


Figure 2. Change of the pressure after the shock, P_s , with the shock position, X_s , for (a) a fixed wavelength of $L = 16$ mm but different amplitudes of $a = 0.2, 0.5$ and 0.8 ; (b) a fixed amplitude of $a = 0.3$ but different wavelengths of $L = 2, 8$ and 16 mm. The dashed black lines correspond to the pressure at the von Neumann state calculated based on the (a) initial local reactant concentration and (b) homogeneous mixture.

3.2 Two-dimensional detonation propagation

Then we consider 2D detonation propagation in the inhomogeneous mixture. Figure 3 shows the numerical soot foils for different L and a . For homogeneous mixture, the detonation propagates at CJ speed, the regular cellular structure develops and the cell size keeps constant. For inhomogeneous mixture, similar to the 1D results, there are critical amplitude a_c and wavelength L_c (detonation quenches for $L = 16$ mm, not shown here), above which detonation quenches and cellular structure disappears. Besides, a much larger cellular structure appears in the inhomogeneous region for fixed $L = 2$ mm but different $a = 0.2$ and 0.3 . The size of the large cellular structure does not change with a and it remains to be around $\lambda = 2.5$ mm. Different to the results for fixed L , Fig 3(b) shows that the large-scale cell size increases with L . The number of triple points adjusts rapidly in the inhomogeneous mixture. For $L = 4$ mm, the large cell size is around $\lambda = 5$ mm, which is one order of magnitude larger than $\lambda_0 = 0.4$ mm for homogeneous mixture. Moreover, in the range of $6.5 \text{ cm} < x < 8 \text{ cm}$ for $L = 4$ mm, substructures appear within the large cellular structure. A similar phenomenon has been found in 1D cases with double periodic propagation of shock (see Fig. 3 with $L_l = 2L$).

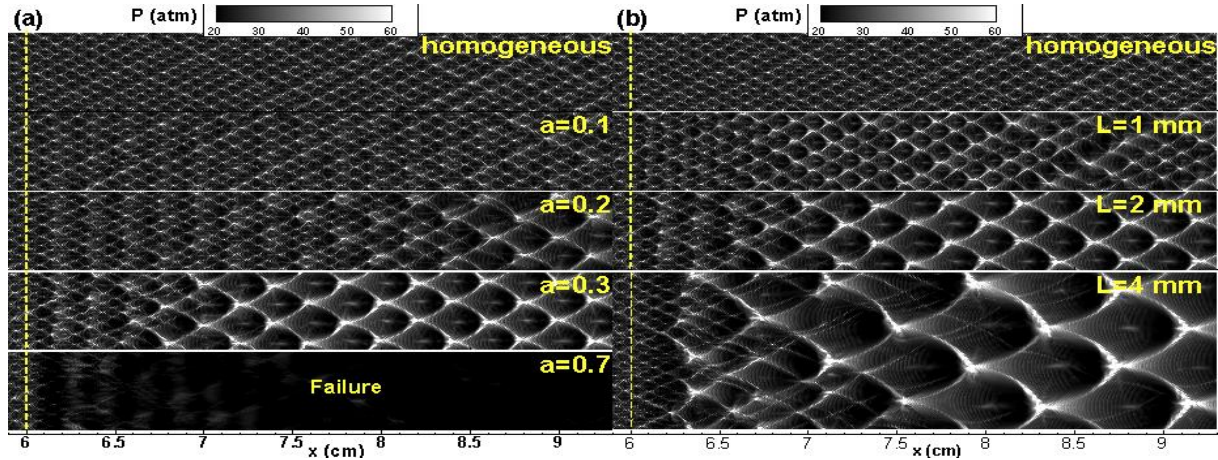


Figure 3. Numerical soot foils for (a) a fixed wavelength of $L = 2$ mm but different amplitudes of $a = 0.1, 0.2, 0.3$ and 0.7 ; (b) a fixed amplitude of $a = 0.3$ but different wavelengths of $L = 1, 2$ and 4 mm. The results for the homogeneous mixture are shown together for comparison.

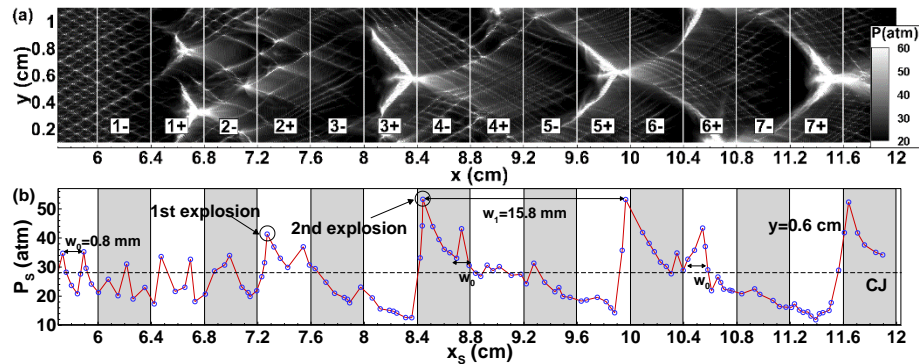


Figure 4. (a) Numerical soot foils and (b) change of the pressure immediately after the leading shock, P_s , with the shock position, X_s , along the line at $y = 0.6$ cm for $L = 8$ mm and $a = 0.3$.

In order to interpret the double cellular structure, the results for $L = 8$ mm and $a = 0.3$ are displayed in Fig. 4. When detonation propagates into the region 1-, the shock pressure decreases and original cellular structure disappears. When the detonation propagates into the region 1+, two local explosions occur around $(x, y) = (6.6$ cm, 0.8 cm) and $(6.7$ cm, 0.3 cm), and the peak shock pressure is recovered as shown in Fig. 4(b). From region 1+ to 2+, detonation reinitiation happens. In region 3-, the shock pressure decreases again and the cellular structure tends to disappear, which is similar to the observation in region 1-. As the detonation propagates in region 3+, a much stronger second local explosion occurs, resulting in an overdriven detonation whose peak pressure is above 50 atm. Then, the large cellular structure with $\lambda_1 \approx 9.6$ mm and $w_1 \approx 15.8$ mm is formed due to the regular movement of secondary triple points. Within the large-scale cellular structure are substructures with $\lambda_0 \approx 0.4$ mm and $w_0 \approx 0.8$ mm, which are due to the movement of the original triple points as in the homogeneous mixture. Such interesting cellular structure was also obtained by [4].

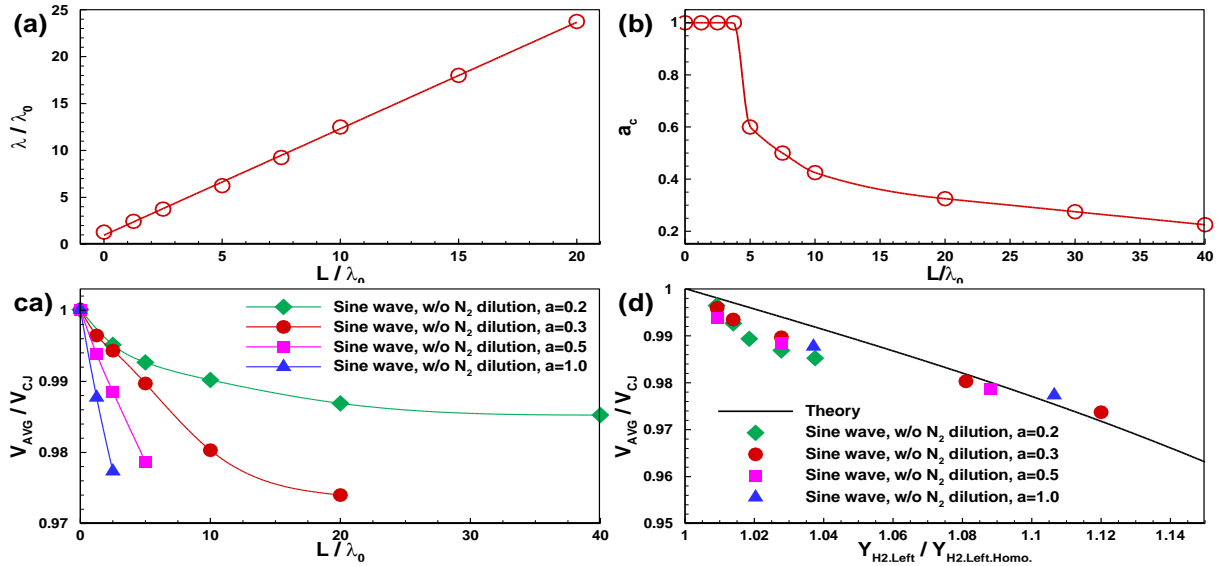


Figure 5. Change of the (a) normalized large cell size, λ/λ_0 ; (b) critical inert layer thickness, a_c ; (c) normalized averaged detonation propagation speed, V_{AVG}/V_{CJ} with the normalized wavelength, L/λ_0 ; (d) Change of the normalized averaged detonation propagation speed, V_{AVG}/V_{CJ} , with the normalized unburned hydrogen mass fraction, $Y_{H_2,Left}/Y_{H_2,Left,Homo}$.

To quantify the properties of detonation propagation in inhomogeneous mixtures, here we study the change of large-scale cell size, critical amplitude and detonation speed deficit shown in Fig. 5. Fig. 5(a) shows that the large cell size increases linearly with L . This is because the large cellular structure is mainly induced by periodic detonation reinitiation, as interpreted by Fig. 4. Fig. 5(b) indicates that The critical amplitude decreases monotonically with the increase of the normalized L . This is because a larger wavelength corresponds to a broader region with high nitrogen concentration and thus the detonation can be quenched more easily. Figure 4(c) shows that the averaged detonation speed is close to the CJ speed since averaged fuel concentration in the inhomogeneous mixture is the same as in the homogeneous mixture (see Eq. 1). Besides, the detonation speed deficit increases with L and a . To interpret the speed deficit in inhomogeneous mixture, we calculated the amount of unburned hydrogen left behind the detonation, $Y_{H_2,Left}$, in the inhomogeneous mixture, and compared it with that in the homogenous mixture, $Y_{H_2,Left,Homo}$. It is found that more unburned hydrogen is left behind the detonation in the inhomogeneous than in the homogenous mixture case, which is the cause for the detonation speed deficit shown in Fig. 5(c). Figure 5(d) plots the

change of the normalized averaged detonation speed versus the normalized unburned hydrogen mass fraction. The solid line is theoretical CJ detonation speed calculated based on reactant concentration. Good agreement between theoretical and simulation results is observed. This demonstrates that detonation speed deficit is due to the amount of unburned fuel left behind the detonation with cellular structure.

4 Conclusions

In this study, 1D and 2D simulations considering detailed chemistry are conducted to investigate the effect of inhomogeneous distribution of reactant concentration on detonation propagation. It was observed that a detonation can be quenched in the inhomogeneous mixture when the amplitude or wavelength of sinusoidal distribution is above certain critical threshold values. The critical amplitude decreases monotonically with the wavelength. For amplitude and wavelength values below their critical thresholds, detonation reinitiation occurs in the inhomogeneous mixtures. Successful reinitiation can be triggered by local autoignition and explosion due to collision of transverse shock waves. There exists a double period of the leading shock pressure propagation for 1D simulations and a double cellular structure consisting of a large-scale structure and smaller substructures, respectively due to the movement of the original and secondary triple points for 2D simulations. The normalized large-scale cell size was found to be linearly proportional to the normalized wavelength. Furthermore, a small detonation speed deficit in the inhomogeneous mixture was found and could be attributed to the amount of unburned fuel left behind the detonation with cellular structure.

Acknowledgements

This work was supported by National Natural Science Foundation of China (Nos. 91541204 & 91741126).

References

- [1] J. Fujii, Y. Kumazawa, A. Matsuo, S. Nakagami, K. Matsuoka and J. Kasahara, Numerical investigation on detonation velocity in rotating detonation engine chamber, *Proc. Combust. Inst.* **36** (2017) 2665-2672.
- [2] A. Teodorczyk and F. Benoit, Interaction of detonation with inert gas zone, *Shock Waves* **6** (1996) 211-223.
- [3] Y. Wang, C. Huang, R. Deiterding, H. Chen and Z. Chen, Propagation of gaseous detonation across inert layers, *Proc. Combust. Inst.* **38** (2021) 3555-3563.
- [4] M.I. Radulescu and B.M. Maxwell, The mechanism of detonation attenuation by a porous medium and its subsequent re-initiation, *J. Fluid Mech.* **667** (2011) 96-134.
- [5] X. Mi, E.V. Timofeev and A.J. Higgins, Effect of spatial discretization of energy on detonation wave propagation, *J. Fluid Mech.* **817** (2017) 306-338.
- [6] G.O. Thomas, P. Sutton and D.H. Edwards, The behavior of detonation waves at concentration gradients, *Combust. Flame* **84** (1991) 312-322.
- [7] S. Boulal, P. Vidal and R. Zitoun, Experimental investigation of detonation quenching in non-uniform compositions, *Combust. Flame* **172** (2016) 222-233.
- [8] W.J. Ma, C. Wang and W.H. Han, Effect of longitudinal concentration gradient on 1-D double-period detonation, *Proceedings of the 27th International Colloquium on the Dynamics of Explosions and Reactive Systems*, Beijing., (2019).
- [9] Z. Chen, Effects of radiation and compression on propagating spherical flames of methane/air mixtures near the lean flammability limit, *Combust. Flame* **157** (2010) 2267-2276.
- [10] R. Deiterding, A parallel adaptive method for simulating shock-induced combustion with detailed chemical kinetics in complex domains, *Computers & Structures* **87** (2009) 769-783.